JACS
JOURNAL OF THE AMERICAN CHEMICAL SOCIETY

Subscriber access provided by American Chemical Society

Article

Proof of Large Positive Zero-Field Splitting in a Ru Paddlewheel

Wei-Zhong Chen, F. Albert Cotton, Naresh S. Dalal, Carlos A. Murillo, Chris M. Ramsey, Tong Ren, and Xiaoping Wang

J. Am. Chem. Soc., **2005**, 127 (36), 12691-12696• DOI: 10.1021/ja053615a • Publication Date (Web): 18 August 2005

Downloaded from http://pubs.acs.org on March 25, 2009

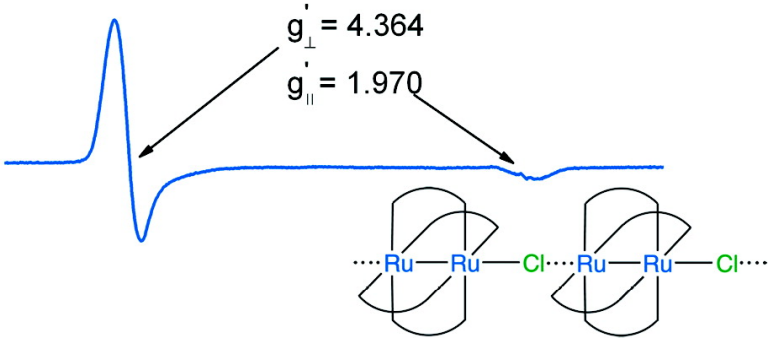

More About This Article

Additional resources and features associated with this article are available within the HTML version:

- Supporting Information
- Links to the 2 articles that cite this article, as of the time of this article download
- Access to high resolution figures
- Links to articles and content related to this article
- Copyright permission to reproduce figures and/or text from this article

View the Full Text HTML

ACS Publications
High quality. High impact.

Journal of the American Chemical Society is published by the American Chemical Society. 1155 Sixteenth Street N.W., Washington, DC 20036

J|A|C|S
ARTICLES
Published on Web 08/18/2005

Proof of Large Positive Zero-Field Splitting in a Ru_2^{5+} Paddlewheel

Wei-Zhong Chen,[†] F. Albert Cotton,*[,‡] Naresh S. Dalal,*[,§] Carlos A. Murillo,*[,‡] Chris M. Ramsey,[§] Tong Ren,*[,†] and Xiaoping Wang[‡]

Contribution from the Department of Chemistry, University of Miami, Coral Gables, Florida 33146, Department of Chemistry and Laboratory for Molecular Structure and Bonding, P.O. Box 30012, Texas A&M University, College Station, Texas 77842-3012, Department of Chemistry and Biochemistry and National High Magnetic Field Laboratory, and Florida State University, Tallahassee, Florida 32306-4390

Received June 2, 2005; E-mail: cotton@tamu.edu; murillo@tamu.edu; dalal@chem.fsu.edu; tren@miami.edu

Abstract: We present the synthesis, as well as the structural and magnetic characterization, of $[Ru_2(D(3,5\text{-}Cl_2Ph)F)_4Cl(0.5H_2O)]\cdot C_6H_{14}$ (D(3,5-Cl_2Ph)F = *N*,*N*′-di(3,5-dichlorophenyl)formamidinate), a Ru_2^{5+} compound having a $^4B_{2u}$ ground state derived from a $\sigma^2\pi^4\delta^2\pi^{*2}\delta^*$ electron configuration. The persistence of this configuration from 27 to 300 K is shown by the invariance of the Ru−Ru distance. Orientation-dependent magnetic susceptibility (χT) and magnetization ($M(H)$) data are in accord with a spin quartet ground state with large magnetocrystalline anisotropy associated with a large axial zero-field splitting (D) parameter. Theoretical fits to χT and $M(H)$ plots yielded $D/k_B = +114$ K, implying an $S = \pm^1/_2$ Kramers doublet ground state at low temperature. Single-crystal and powder EPR data are consistent with this result, as the only observed transition is between the $M_s = \pm^1/_2$ Zeeman levels. The g values are $g_\perp = 2.182$, $g_\parallel = 1.970$, and $D = 79.8$ cm^{-1}. The totality of the results demands $D \gg 0$.

The discovery of compounds containing the Ru_2^{5+} core surrounded by bridging bidentate ligands (the weakly basic carboxyl anions having been the first) in a paddlewheel pattern dates back to 1966.[1] However, the presumed paddlewheel structure was not confirmed until 1969,[2] when the very short Ru−Ru distance of 2.281(4) Å at 279 K was determined, and the presence of strong metal−metal bonding was thus affirmed.

In 1975, the first study of the magnetic properties (bulk susceptibility and EPR spectrum) of $Ru_2(O_2CC_3H_7)_4Cl$ was reported.[3] To account for the magnetic properties, it was proposed that the π^* and δ^* orbitals of the Ru_2^{5+} core were so close in energy (a situation not previously suggested for metal−metal multiple bonds) that three electrons were spread out over both orbitals, thus creating a $^4B_{2u}$ ground state for the molecule. The magnetic results were interpreted quantitatively in terms of a large zero-field splitting and an axial spin Hamiltonian. About a decade later, the essential results of this study were verified,[4] although, based on new data at lower temperatures, numerical parameters were altered to $D = 77$ cm^{-1}, $g_\parallel = 2.03$, and $g_\perp = 2.18$. It was also concluded that, even though the structure consists of infinite zigzag chains of $Ru_2(O_2CC_3H_7)_4$-Cl with bent but symmetrical Ru−Cl−Ru bridges, interaction between Ru_2^{5+} units is negligible.

The first rigorous calculations for Ru_2^{5+} (as well as for Ru_2^{4+}) carboxylate compounds were published in 1979 by Norman, Renzoni, and Case.[5] These calculations confirmed the previously proposed near-degeneracy of the π^* and δ^* orbitals for both Ru_2^{5+} and Ru_2^{4+} species, and were consistent with previous interpretations of magnetic results.

For Ru_2^{4+} compounds of the types $Ru_2(O_2CR)_4$ and $Ru_2(O_2CR)_4L_2$, theoretical results for R = H predicted either a $\sigma^2\pi^4\delta^2\pi^{*3}\delta^*$ configuration[5] or a $\sigma^2\pi^4\delta^2\delta^{*2}\pi^{*2}$ configuration,[6] but in neither case are the results unequivocal, and the possible dependence on the identity of R has not been explored. It may be noted that, for R = CH_3, a magnetic study demonstrated that the $\sigma^2\pi^4\delta^2\delta^{*2}\pi^{*2}$ configuration (giving rise to a $^3A_{2g}$ ground state) is correct.[7]

Since the early work, a very large number of compounds containing Ru_2^{5+} cores, as well as quite a few with Ru_2^{4+} and Ru_2^{6+} cores, have been reported.[8] In addition to carboxyl groups, bridging ligands having N,O and N,N pairs of donor atoms have been extensively used. It was recognized a long time ago[9] that N,N ligands may differ a lot from carboxyl groups in their influence on the relative energies of the Ru−Ru bonding and antibonding orbitals. Because of the difficulties often associated

[†] University of Miami.
[‡] Texas A&M University.
[§] Florida State University.

(1) Stephenson, T. A.; Wilkinson, G. *J. Inorg. Nucl. Chem.* **1966**, *28*, 2285.
(2) Bennett, M. J.; Caulton, K. G.; Cotton, F. A. *Inorg. Chem.* **1969**, *8*, 1.
(3) Cotton, F. A.; Pedersen, E. *Inorg. Chem*. **1975**, *14*, 388.
(4) Telser, J.; Drago, R. S. *Inorg. Chem.* **1984**, *23*, 3114.
(5) Norman, J. G., Jr.; Renzoni, G. E.; Case, D. A. *J. Am. Chem. Soc.* **1979**, *101*, 5256.
(6) Clark, D. L.; Green, J. C.; Redfern, C. M.; Quelch, G. E.; Hillier, I. H.; Guest, M. F. *Chem. Phys. Lett.* **1989**, *154*, 326.
(7) Cotton, F. A.; Miskowski, V. M.; Zhong, B. *J. Am. Chem. Soc.* **1989**, *111*, 6177.
(8) Angaridis, P. In *Multiple Bonds Between Metal Atoms*, 3rd ed.; Cotton, F. A., Murillo, C. A., Walton, R. A., Eds.; Springer Science and Business Media, Inc.: New York, 2005.
(9) Cotton, F. A.; Matusz, M. *J. Am. Chem Soc.* **1988**, *110*, 5761.

with determining the relative energies of the orbitals, simply writing ($\pi^*\delta^*$) for the outmost energy levels of the Ru_2^{5+} species has become common practice.

However, recent studies[10,11] in one of our laboratories have shown that important, and otherwise inaccessible, information on the electronic states of Ru_2^{6+} and Ru_2^{5+} compounds, and how these states depend on temperature, may be obtained by measuring the temperature dependence of the Ru−Ru distance over a wide range from about 300 K to about 27 K. In this way, magnetic changes that are due only to zero-field splitting with no change in electron configuration can be unambiguously distinguished from those that are due to a Boltzmann-type temperature dependence of electronic configuration, because Ru−Ru distances remain invariant in the former case while changes are expected in the latter situation.

It should be noted that compounds containing one Ru_2^{5+} core (or several[12−14]) might have liquid crystalline applications,[15] may be incorporated into magnetic polymeric assemblies,[12] or may be building blocks for large magnetic supramolecular clusters,[13,14,16] and even for 3-D[17] or 2-D[18] molecule-based magnets. However, it is clear that understanding the subtle factors that determine the electronic configuration of an individual Ru_2^{5+} unit is a prerequisite to understanding what goes on in larger arrays. The latter may also exhibit unusually large magnetic anisotropy, which is characterized by the zero-field splitting parameter, D, as already shown.[3,11] In these systems, D tends to be the factor that dominates the overall magnetic behavior. Thus, it is very important to determine both the magnitude and the sign of the zero-field splitting parameter for use in magnetic applications. In previous work[3,11,19] D has been assumed to be positive, but we present here definitive proof of this. Specifically, single-crystal, orientation-dependent magnetic susceptibility (χT) and magnetization ($M(H)$) measurements have been carried out on the compound $[Ru_2(D(3,5\text{-}Cl_2Ph)F)_4Cl(0.5H_2O)]\cdot C_6H_{14}$ (**1**). In this way it is possible to probe its spin Hamiltonian parameters and unambiguously determine the sign of D. Ambiguity about the sign of D has arisen because previously reported χT and $M(H)$ measurements were for powder samples only. Kahn has pointed out[20] that, while the calculated χT vs T curves for the parallel and perpendicular field orientations are drastically different for the $D > 0$ and $D < 0$ cases, their powder averages are very similar. This makes it possible for the other fitting parameters, $g_{\parallel}$ and $g_{\perp}$, to absorb the small differences, resulting in a loss of information concerning the absolute sign of the zero-field splitting. In the present report, we provide comprehensive data and insight into the properties of a Ru_2^{5+} compound that is exceptionally well suited to provide a definitive understanding of the $^4B_{2u}$ state arising from a $\pi^{*2}\delta^*$ configuration which persists over the entire temperature range from 3 to 300 K.

Experimental Details

A. Preparation of $[Ru_2(D(3,5\text{-}Cl_2Ph)F)_4Cl(0.5H_2O)]\cdot C_6H_{14}$ (1). In this procedure,[21] a round-bottom flask was charged with $Ru_2(OAc)_4Cl$ (0.24 g, 0.50 mmol), *N*,*N*′-di(3,5-dichlorophenyl)formamidine (1.35 g, 4.0 mmol), LiCl (0.4 g), Et_3N (2 mL), and 50 mL of THF. The mixture was gently refluxed under argon for 4 days. The color of the reaction mixture turned violet upon refluxing. After the removal of solvents from the reaction mixture, the residue was treated with warm ethanol (3 × 60 mL). The residue was then recrystallized from warm CH_2Cl_2/ethanol solution to yield 0.64 g of a black crystalline material (82% based on Ru). Analysis for $Ru_2C_{52}H_{28}Cl_{17}N_8\cdot H_2O\cdot C_6H_{14}$, found (calcd): C, 41.07 (41.34); H 2.51 (2.60); N, 6.77 (6.73). UV−vis data, λ_{max} (nm, ϵ (M^{-1} cm^{-1})): 601 (3340), 494 (6530), 271 (46 900). IR (cm^{-1}, KBr disk): 1581(m), 1567(s), 1535(s), 1425(m), 1330(m), 1252(w), 1220(w), 1112(w), 1097(w), 1005(m), 939(m), 854(w), 807(m), 731(w), 700(w), 678(w), 661(w), 541(w), 455(w), 433(w).

B. Magnetic Susceptibility Measurements. Direct current magnetic susceptibility and magnetization measurements were performed on a Quantum Design MPMS XL7 (SQUID) magnetometer. The sample temperature was varied from 1.8 to 300 K and the static field from 0 to 7 T. Static measuring fields of 0.1 T were employed for the temperature-dependent measurements. A single crystal was oriented under a microscope in a low-susceptibility plastic sample holder for orientation-dependent measurements. The diamagnetic contribution from the sample holder was carefully determined and subsequently subtracted.

C. EPR Measurements. Variable-temperature X-band (~9.5 GHz) EPR data were recorded on a Bruker E500 spectrometer equipped with a continuous-flow Oxford X-band liquid He cryostat. Temperatures were varied between 300 and 1.8 K. A calibrated NMR teslameter was used for accurate magnetic field measurements. The frequency was recorded to six digits with a built-in digital frequency counter. The single-crystal alignment was controlled with a computerized goniometer.

D. X-ray Crystallography. A Bruker SMART 1000 X-ray three-circle diffractometer was employed for data collection following a previously published procedure.[10] Low-temperature measurements of the single-crystal structure at 27, 100, and 300 K were achieved with the use of an Oxford Helix cooling system. Space group of *P*4/*ncc* (No. 130) for **1** was determined according to the systematic reflection conditions. The structure was solved by direct methods.[22] Non-hydrogen atoms except those of the hexane of solvation were refined with anisotropic thermal parameters. Hydrogen atoms were placed in idealized positions. The structure was refined (weighted least-squares refinement on F^2) to convergence. One of the phenyl groups was disordered over two positions (68/32) and modeled with distance restraints. The half-occupied water molecule resides on a crystallographic four-fold axis. The disordered hydrogen atoms on the water molecule were placed on calculated positions in accordance with the crystal symmetry. Isomeric hexanes of solvation were found disordered about a crystallographic two-fold axis. The disordered hexanes were refined with distance constraints. Selected bond lengths and angles are listed in Table 1. Crystal data and structure parameters at the measured temperatures are given as Supporting Information.

Results

A. Crystal Structure. A drawing of **1** at 27 K is shown in Figure 1, where the paddlewheel arrangement of four D(3,5-

(10) Cotton, F. A.; Murillo, C. A.; Reibenspies, J. H.; Villagrán, D.; Wang, X.; Wilkinson, C. C. *Inorg. Chem.* **2004**, *43*, 8373.
(11) Angaridis, P.; Cotton, F. A.; Murillo, C. A.; Villagrán, D.; Wang, X. *J. Am. Chem. Soc.* **2005**, *127*, 5008.
(12) Miyasaka, H.; Clérac, R.; Campos-Fernández, C. S.; Dunbar, K. R. *Inorg. Chem.* **2001**, *40*, 1663.
(13) Angaridis, P.; Berry, J. F.; Cotton, F. A.; Murillo, C. A.; Wang, X. *J. Am. Chem. Soc.* **2003**, *125*, 10327.
(14) Angaridis, P.; Berry, J. F.; Cotton, F. A.; Lei, P.; Lin, C.; Murillo, C. A.; Villagrán, D. *Inorg. Chem. Commun.* **2004**, *7*, 9.
(15) (a) Cukiernik, F. D.; Luneau, D.; Marchon, J.-C.; Maldivi, P. *Inorg. Chem.* **1998**, *37*, 3698. (b) Cayton, R. H.; Chisholm, M. H.; Darrington, F. D. *Angew. Chem., Int. Ed. Engl.* **1990**, *29*, 1481.
(16) Angaridis. P.; Cotton, F. A.; Murillo, C. A.; Villagrán, D.; Wang, X. *Inorg. Chem.* **2004**, *43*, 8290.
(17) Vos, T. E.; Liao, Y.; Shum, W. W.; Her, J.-H.; Stephens, P. W.; Reiff, W. M.; Miller, J. S. *J. Am. Chem. Soc.* **2004**, *126*, 11630.
(18) Vos, T. E.; Miller, J. S. *Angew. Chem., Int. Ed.* **2005**, *44*, 2416.
(19) See for example: (a) Jiménez-Aparicio, R.; Urbanos, F. A.; Arrieta, J. M. *Inorg. Chem.* **2001**, *40*, 613. (b) Barral, M. C.; González-Prieto, R.; Jiménez-Aparicio, R.; Priego, M. R.; Torres, M. R.; Urbanos, F. A. *Eur. J. Inorg. Chem.* **2003**, 2339. (c) Barral, M. C.; Jiménez-Aparicio, R.; Pérez-Quintanilla, D.; Priego, J. L.; Royer, E. C.; Torres, M. R.; Urbanos, F. A. *Inorg. Chem.* **2000**, *39*, 65.
(20) Kahn, O. *Molecular Magnetism*; VCH: New York, 1993.
(21) Lin, C. Ph.D. Dissertation, Florida Institute of Technology, 1997.
(22) Sheldrick, G. M. *SHELXTL V6.12*; Bruker AXS Inc.: Madison, WI, 2001.

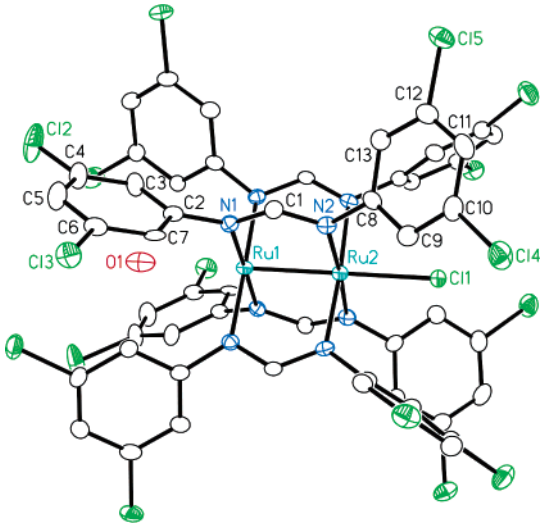

Figure 1. Structure of $Ru_2(D(3,5\text{-}Cl_2Ph)F)_4Cl(0.5H_2O)$ in **1**, with non-disordered atoms shown as displacement ellipsoids at the 30% probability level. Only one of the disordered conformers is shown. H atoms are omitted for clarity.

Table 1. Selected Interatomic Distances (Å) and Angles (deg) for **1** at Various Temperatures

	temperature		
	27 K	100 K	300 K
Ru1−Ru2	2.360 (1)	2.363(1)	2.368(1)
Ru2−Cl1	2.379(3)	2.382(3)	2.381(3)
Ru1···O1	2.63(3)	2.63(3)	2.74(3)
Ru1−N1	2.056(5)	2.053(5)	2.062(5)
Ru2−N2	2.104(5)	2.104(5)	2.097(5)
N1−Ru1−Ru2	90.4(1)	90.6(1)	90.5(1)
N2−Ru2−Ru1	88.1(1)	88.1(1)	88.1(1)

$Cl_2Ph)F$ ligands around the Ru_2 core is clear. The crystallographic four-fold axis coincides with the Cl1−Ru2−Ru1−O1 vector and relates the independent D(3,5-Cl_2Ph)F ligand (labeled with N1 and N2) to the other three. Selected bond lengths and angles for structures determined for **1** at 27, 100, and 300 K are listed in Table 1. The Ru−Ru bond length in **1** (2.360(1) Å) at 27 K is slightly shorter than that of $Ru_2(DTolF)_4Cl$,[23] while the Ru−N distances in **1** are slightly elongated. It is noteworthy that the Ru−Cl bond in **1** (2.379(3) Å) is shortened by 0.033 Å from that of $Ru_2(DTolF)_4Cl$, which can be attributed to lower electron density in the antibonding orbitals ($\delta^*\pi^*$) of the Ru_2 core of **1**. A result of major importance, however, is that there is no significant change in the Ru−Ru distance over the entire range of measured temperatures, 27−300 K.

In addition to the structure of the individual molecule, the packing of these molecules in the crystal is of prime importance. The crystals are tetragonal, and the Ru−Ru axes of all molecules are parallel to one another and aligned with the *c* axis of the unit cell, as shown in Figure 2. Because of the bulk of the surrounding ligands, the paramagnetic Ru_2^{5+} units are well separated (11.2 Å distance between nearest neighbors as well as long intermolecular Cl-to-Ru contacts), and magnetic dipole−dipole interactions between them are very weak. Moreover, it is easy to obtain relatively large crystals with well-developed, low-index faces (Figure 2a). Thus, this compound is well suited

(23) Cotton, F. A.; Ren, T. *Inorg. Chem.* **1995**, *34*, 3190.

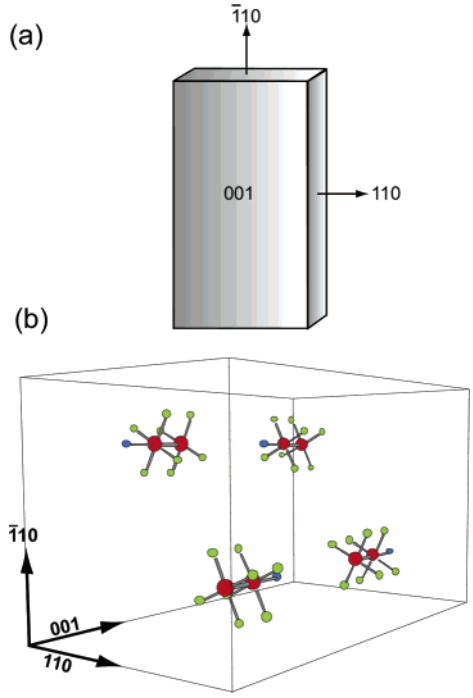

Figure 2. (a) Relationship between the crystal morphology and unit cell axes. (b) The four-fold symmetry direction lies along the 001 axis.

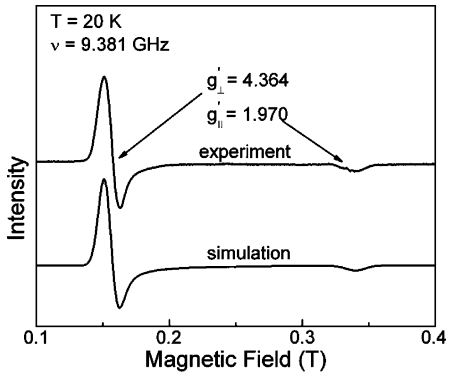

Figure 3. X-band EPR spectrum measured on a powder sample at 20 K, indicating that the unpaired spins are in an axial environment (top trace). The experimental spectrum was simulated (bottom trace) using $S = {}^1/_2$ and the effective *g*-values shown.

for the study of EPR and bulk magnetism by using oriented single crystals.

B. EPR Spectra. Spectra were measured on both powder and a single crystal. Because EPR spectra were not observable above about 150 K due to significant line broadening, most of our measurements were performed at 20 K. This line broadening might be attributed to fast relaxation from the thermally populated $M_S = \pm{}^3/_2$ Zeeman levels. The powder EPR spectrum measured at 20 K and $\gamma = 9.381$ GHz is shown in Figure 3. Two *g*-tensor components are evident, indicating that the electrons reside in an axial environment as expected from the four-fold molecular symmetry. Presumably, the hyperfine components, together with the $I = 0$ transition, are contained within the 120 and 140 G line widths of the perpendicular and parallel features, respectively. Neglecting hyperfine contributions, the simulated[24] 20 K powder spectrum (lower plot of

(24) EPR spectral simulations were performed using Bruker's XSophe software package employing matrix diagonalization techniques.

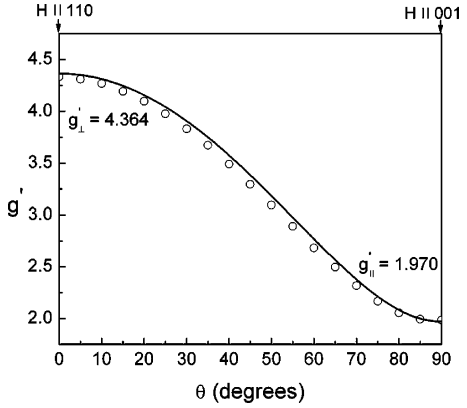

Figure 4. Angular dependence of the single-crystal X-band spectra with the crystal rotated between the perpendicular and parallel axes. The solid line is the simulated behavior based on the powder *g*-values and eq 1. Because the interstitial solvent is evanescent, this result is used to confirm the quality of the powder-determined *g*-values.

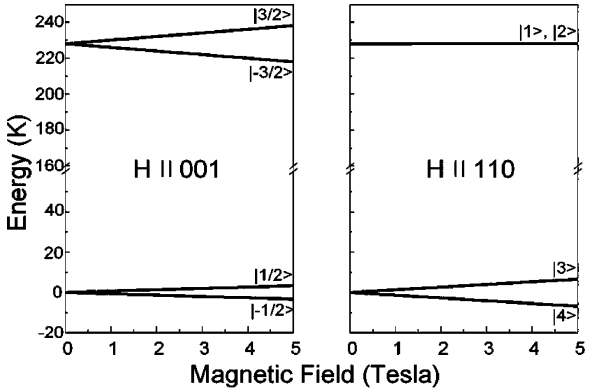

Figure 5. Zeeman energy levels for the field aligned along the 001 (parallel) and 110 (perpendicular) axes.

Figure 3) yields an acceptable fit to the data, with $g_\perp' = 4.364$ and $g_\parallel' = 1.970$. Such large anisotropy provides evidence for the occurrence of significant zero-field splitting. For this reason, these values are labeled with prime symbols, denoting that they are only effective values. For very large D and $S = {}^3/_2$, the effective and actual g-values are related by $g_\perp = g_\perp'/2$ and $g_\parallel = g_\parallel'$.[25] Therefore, the actual values are $g_\perp = 2.182$ and $g_\parallel = 1.970$.

Since interstitial hexane solvent might easily have been lost from the powder sample, the powder data were confirmed through single-crystal angular dependence studies. The results are shown in Figure 4, along with a plot of eq 1 for the angular dependence of g[26] using the $g_\perp' = 4.364$ and $g_\parallel' = 1.970$ parameters taken from the powder results. The agreement

$$g'^2 = g_\perp'^2 \cos^2(\theta) + g_\parallel'^2 \sin^2(\theta) \qquad (1)$$

between the experimental single-crystal data and the expected behavior indeed confirms that the powder *g*-values are appropriate to use as fitting parameters in the single-crystal χT and $M(H)$ measurements. The EPR results do not help to determine the precise magnitude of D, but they do show that $D \gg h\nu$. Higher frequency measurements up to 95 GHz resulted in identical spectra. Therefore, the only conclusion that can be drawn from the EPR data regarding the D parameter is that $D \gg h$(95 GHz) or $D/k_B \gg 4.6$ K. We observed also that the spectra intensify with decreasing temperature, which is consistent with the $M_S = \pm{}^1/_2$ levels lying lower in energy than $\pm{}^3/_2$ and suggesting $D > 0$.

The *g*-values obtained are in line with those calculated by Norman et al.[5] for $Ru_2(O_2CR)_4^+$ complexes based on the proposed $\sigma^2\pi^4\delta^2(\delta^*\pi^*)^3$ molecular orbital scheme for Ru_2^{5+}. In that case, the *g*-values were semiquantitatively calculated using the spin−orbit coupling perturbation to connect the excited and ground states, whose energies and symmetries were obtained by self-consistent field methods. Norman and co-workers determined $g_\perp = 2.18$ and $g_\parallel = 1.97$, in excellent agreement with $g_\perp = 2.182$ and $g_\parallel = 1.970$ determined here for $[Ru_2(D(3,5\text{-}Cl_2Ph)F)_4Cl(0.5H_2O)]\cdot C_6H_{14}$.

C. Bulk Magnetic Properties. The macroscopic crystal morphology was obtained by standard indexing procedures and is shown in Figure 2a. The four-fold molecular symmetry axis lies along 001, and the parallel, or "easy-axis", magnetic behavior should be observed when the field is aligned with the 001 face of the crystal. Moreover, interdimer magnetic exchange interactions should be very small due to a large 11.2 Å distance between nearest neighbors as well as long 8.78 Å Cl−Ru nearest-neighbor contacts. For this reason, the shape of χT vs T was expected to be determined by the molecular symmetry rather than the bulk magnetism.

The magnetic properties of an axially symmetric system with $S = {}^3/_2$, $D \neq 0$, having axial symmetry, may be derived from the spin Hamiltonian in eq 2,[14,27,28] where β is the Bohr

$$\mathscr{H} = \beta\vec{H}\cdot\tilde{g}\cdot\hat{S} + D\{\hat{S}_z^2 - S(S+1)/3\} \qquad (2)$$

magneton, $\vec{H}$ is the magnetic field vector, $\tilde{g}$ is the *g*-tensor, $\hat{S}$ is the spin operator, D is the axial zero-field splitting energy, and S is the total spin of the system. With the axial symmetry direction designated as parallel, diagonalization of this Hamiltonian leads to the parallel and perpendicular energy levels. For the $H_\parallel$ orientation ($H \parallel 001$), $E_{|+1/2\rangle} = g_\parallel\beta H_\parallel/2$, $E_{|-1/2\rangle} = -g_\parallel\beta H_\parallel/2$, $E_{|+3/2\rangle} = 2D + 3g_\parallel\beta H_\parallel/2$, and $E_{|-3/2\rangle} = 2D - 3g_\parallel\beta H_\parallel/2$. For the $H_\perp$ orientation, $E_{|1\rangle} = E_{|2\rangle} = 2D + g_\perp^2\beta^2H_\perp^2/8D$, $E_{|3\rangle} = g_\perp\beta H_\perp - 3g_\perp^2\beta^2H_\perp^2/8D$, and $E_{|4\rangle} = -g_\perp\beta H_\perp - 3g_\perp^2\beta^2H_\perp^2/8D$. The magnetic field dependence for each of these levels is shown in Figure 5. From these energies, the temperature dependence of the parallel and perpendicular susceptibilities as well as the field dependence of the magnetization may be derived. It is clear from the χT vs T data shown in Figure 6 for a single crystal oriented in both the parallel and perpendicular directions with respect to the magnetic field that the anisotropy is quite large. This is consistent with appreciable zero-field splitting. To estimate the magnitude of D and determine its absolute sign, these data were fit to the standard equations describing the susceptibility[20,27] for the two orthogonal axial symmetry orientations (see solid lines in Figure 6). In practice, the parallel susceptibility was obtained by orienting the 001 axis of the

(25) Weltner, W., Jr. *Magnetic Atoms and Molecules*; Van Nostrand-Reinhold: New York, 1983.
(26) Weil, J. A.; Bolton, J. R.; Wertz, J. E. *Electron Paramagnetic Resonance: Elementary Theory and Practical Applications*; John Wiley & Sons: New York, 1994.
(27) Abragam, A.; Bleaney, B. *Electron Paramagnetic Resonance of Transition Ions*; Clarendon Press: Oxford, 1970.
(28) Pilbrow, J. R. *Transition Ion Electron Paramagnetic Resonance*; Clarendon Press: Oxford, 1990.

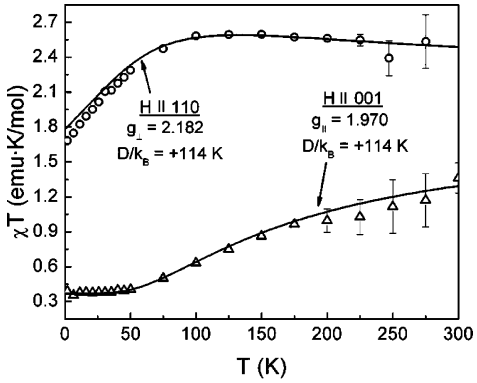

Figure 6. χT vs T for the field aligned parallel to the 001 and 110 axes of the crystal. The solid lines are fits to eqs 3 and 4 with the indicated parameters. The measuring field was 0.1 T.

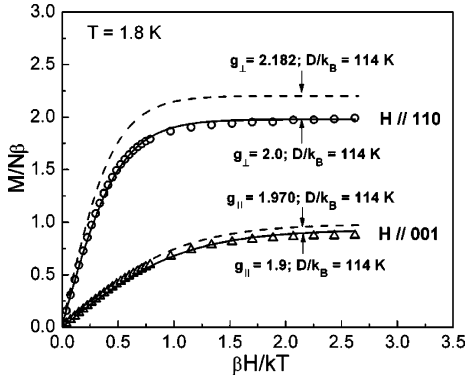

Figure 7. Saturation magnetization data $M(H)$ for the field aligned parallel to the 001 (parallel) and 110 (perpendicular) axes of the crystal. The solid lines are best fits to eqs S4 and S5 (Supporting Information) with the indicated parameters. The dashed lines denote the expected behavior based on the EPR g-values.

crystal parallel to the applied field ($H \parallel 001$). By fixing $g_{\parallel}$ and $g_{\perp}$ to their EPR values and allowing D to vary, a fit to eq 3 gives good agreement with $g_{\parallel} = 1.970$ and $D/k_B = 114$ K.

$$\chi_{\parallel}T = \frac{Ng_{\parallel}^2\beta^2}{4k_B}\left(\frac{1 + 9\exp(-2D/k_BT)}{1 + \exp(-2D/k_BT)}\right) \quad (3)$$

$$\chi_{\perp}T = \frac{Ng_{\perp}^2\beta^2}{k_B}\left(\frac{1 + (3k_BT/4D)(1 - \exp(-2D/k_BT)}{1 + \exp(-2D/k_BT)}\right) \quad (4)$$

Similarly, the results of fitting the $H_{\parallel}$ 110 data with eq 4 yielded $g_{\perp} = 2.182$ and $D/k_B = 114$ K. This large D is consistent with those found in other Ru_2^{5+} complexes. For example, $D/k_B =$ 111 K for $Ru_2(butyrate)_4Cl$,[3] 71.2 K for $Ru_2(DTolF)_4Cl$,[23] 101 K for $Ru_2(DAniF)_3(O_2CCH_3)Cl$[14] (the ligand DAniF is *N*,*N*′-di-*p*-anisylformamidinate), 86 K for $[Ru_2(DAniF)_3Cl]_2(O_2CC_6H_4CO_2)$,[14] and 100 K[29] for $Ru_2(acetate)_4Cl$ and $[Ru_2(acetate)_4]_3[Co(CN)_6]$.

Measurements of the field dependence of the magnetization were performed on the same crystal in both orientations to confirm the large χT anisotropy and that $D > 0$. The energy levels discussed previously were used for theoretical modeling of the magnetization. However, in the case where $g\beta H/k_BT$ is large, the calculation procedure is slightly more tedious than that for evaluating the susceptibility, as Van Vleck's approximation is not applicable in the saturation field regime.[20] Equations for $M_{\parallel}$, the parallel magnetization, and $M_{\perp}$, the perpendicular magnetization, are determined from the partition functions for the two orientations. Equations describing the magnetization of $S = {}^3/_2$ systems with zero-field splitting have been presented before.[29] Those which we derive in slightly different notation are given as Supporting Information. Since our crystals are tetragonal, the rhombic zero-field splitting parameter E has been set equal to zero.

Figure 7 shows the results of magnetization measurements with the field aligned along the 001 and 110 axes of the single crystal. Using the standard formula for paramagnetic saturation,[30] $M/N\beta = gS$, it is clear that, for an $S = {}^1/_2$ system, the magnetization should approach $M/N\beta = 1.0$ if $g = 2$. While the parallel ($H_{\parallel}$ 001) magnetization seems to approach this value, the perpendicular ($H_{\parallel}$ 110) magnetization saturates at twice this amount, as if $g = 4$. Therefore, while the $M_S = \pm{}^3/_2$ levels are not appreciably populated at 1.8 K, there is significant mixing of the energy levels via off-diagonal matrix elements in the perpendicular direction.

It should be noted that the data of Figure 7 were well-fit by eqs S4 and S5 (see Supporting Information) with the parameters $g_{\parallel} = 1.90$, $g_{\perp} = 2.00$, and $D/k_B = 114$ K. Because $D \gg k_BT$ at 1.8 K, these fits were relatively insensitive to the magnitude of D/k_B, and for this reason, it was not a fitting parameter. The g-values obtained from this fitting procedure are slightly lower than those obtained by EPR. The dashed lines indicate the expected magnetization curve using the EPR values $g_{\parallel} = 1.970$ and $g_{\perp} = 2.182$. For the experimental perpendicular magnetization ($H \parallel 110$), the data reach 1.99 at 7 T, which is 88% of the expected value of 2.25. Similarly, the parallel magnetization reaches 0.89 at 7 T, only 92% of the expected 0.97.

The fact that the g-values obtained from this fitting procedure are slightly lower than those obtained by EPR means that the observed magnetization is reduced by a small factor, as compared to that projected from the g-factors. This discrepancy can be attributed to at least two mechanisms. First, one can add additional terms in the spin Hamiltonian, as for example the E term if we include the effect (however small) of the solvent disorder. Second, addition of interdimer antiferromagnetic interactions could account for a lowering of the magnetization by a few percent. In any case, the cause of this discrepancy is uncertain at this point.

Discussion

It has been shown in a recent report[11] on the compounds $Ru_2[(m\text{-anisylN})_2CH]_4Cl$ and $Ru_2[(p\text{-anisylN})_2CH]_4Cl$ that their electronic structures are qualitatively different owing to the different inductive effects of *m*-anisyl (electron-withdrawing, Hammett $\sigma = +0.12$) and *p*-anisyl (electron-donating, Hammett $\sigma = -0.27$) groups. It was concluded that the *m*-anisyl compound has a $\pi^{*2}\delta^*$ electron configuration at temperatures between 3 and 300 K, and accordingly, its Ru−Ru distance is invariant from 27 to 300 K. However, its χT value drops between 300 and 3 K in the expected manner based on zero-field splitting of a $^4B_{2u}$ state arising from the $\pi^{*2}\delta^*$ electronic configuration.

One purpose of the present study was to take advantage of a fortunate combination of circumstances. First the 3,5-dichloro-

(29) Shum, W. W.; Liao, Y.; Miller, J. S. *J. Phys. Chem. A* **2004**, *108*, 7460.
(30) Carlin, R. L. *Magnetochemistry*; Springer-Verlag: Berlin, 1986.

phenyl group ($\sigma = 0.74$) is even more electron-withdrawing than the *m*-anisyl group. Second, the compound forms tetragonal crystals in which all the molecules are aligned parallel, the crystals grow relatively large, and they show well-developed, low-index faces which are helpful in orienting single crystals.

The structure of the 3,5-dichloro compound shows its qualitative similarity to the *m*-anisyl homologue. The Ru−Ru distance is, again, invariant with temperature and not very different (2.368(1) Å at 300 K). This, together with the magnetic data, shows that the 3,5-dichloro compound has a $\pi^{*2}\delta^*$ configuration throughout the temperature range 3−300 K. The 3,5-dichloro compound therefore provides an unprecedented opportunity to explore the consequences of this electronic configuration in exquisite detail.

As shown in Figure 6, by magnetic anisotropy measurements it was established very directly that $g_\perp = 2.182$ and $g_\parallel = 1.970$ and that the zero-field splitting of the $^4B_{2u}$ state arising from the $\pi^{*2}\delta^*$ configuration is 114 K (equivalent to 79.8 cm^{-1}). More important still, it is now proven, unequivocally, that the zero-field splitting parameter, *D*, is positive. This assumption has been made in the past, and while it seemed unlikely to be wrong, direct proof of its correctness is important.

Finally, EPR data for the 3,5-dichloro compound (Figures 3 and 4) clearly confirm that, as required by $D \gg 0$, the $M_S = \pm^1/_2$ Kramers doublet lies well below the $M_S = \pm^3/_2$ doublet and that the spin Hamiltonian is axial. The EPR data also verify, quantitatively, the *g* values derived from the magnetic susceptibility measurements.

All of the magnetic and EPR results obtained here for the 3,5-dichloroformamidinate compound are consonant with those for $Ru_2(O_2CC_3H_7)_4Cl$, despite the fact that the Ru−Ru distance in the latter (2.281(4) Å) is appreciably shorter than the present one (2.368(1) Å). A comparison of key magnetic parameters for the two compounds, presented in Table 2, shows that near-degeneracy of the δ^* and π^* orbitals is common to both compounds. However, this need not, and probably does not, mean that the entire manifold of molecular orbitals that provide the Ru−Ru as well as the Ru−ligand bonding is similar for the two compounds. This would be a priori unlikely, given the differences between RCO_2^- and $ArNC(H)NAr^-$ ligands, as well as the observed structural differences (e.g., in the Ru−Ru distances). The magnetic properties of both compounds are, however, quite similar because they depend mainly on the relative energies and populations of the δ^* and π^* orbitals.

Table 2. Comparison of $Ru_2(O_2CC_3H_7)_4Cl$ (**A**) and $Ru_2[D(3,5\text{-}Cl_2Ph)F]_4Cl$ (**B**)

	A	B
Ru−Ru, Å, at ca. 300 K	2.281(1)	2.368(1)
$g_\perp$	2.135	2.182
$g_\parallel$	2.022	1.970
D, cm^{-1}	76.8	79.8

Acknowledgment. We thank the National Science Foundation (CHE-0242623 to T.R., DMR/NIRT-0103290 to N.S.D. and CHE-457031 to F.A.C.) and the Robert A. Welch Foundation for support. We also thank Dr. W. Wernsdorfer, CRNS, Grenoble, France for helpful discussions.

Supporting Information Available: X-ray crystallographic files for $[Ru_2(D(3,5\text{-}Cl_2)PhF)_4Cl(0.5H_2O)]\cdot C_6H_{14}$ (CIF); derivation of equations for the field dependence of the magnetization (PDF). This material is available free of charge via the Internet at http://pubs.acs.org.

JA053615A